Meningococcal PorA/C1, a Channel that Combines High Conductance and High Selectivity

Jinming Song,* Conceição A.S.A. Minetti,# M. S. Blake,# and Marco Colombini*
*University of Maryland, Department of Biology, College Park, Maryland 20742 and #North American Vaccine, Inc., Columbia, Maryland 21046 USA

ABSTRACT Class 1 porins (PorA/C1) from *Neisseria meningitidis* achieve both high selectivity and high conductance. The channel is highly selective (24:1 Na^+ over Cl^-), suggesting a highly negatively charged selectivity filter. The trimeric nature of PorA/C1 accounts for part of the enormous conductance in 200 mM NaCl (0.97nS). However, the currents that can be achieved exceed the simple infinite-sink calculation for a pore 0.7 nm in radius (estimated from nonelectrolyte permeability). The conductance is linear with salt activity from 20 mM to 2.0 M NaCl with no sign of saturation at low salt. Impermeant polymers reduce the conductance in a manner consistent with their ability to reduce bulk conductivity. Extrapolating from the known structure of homologous porins, the selectivity filter is likely to be small and localized. If small and highly negatively charged (~9 charges), the predicted conductance would be an order of magnitude higher than that observed. The rate at which ions reach the selectivity filter seems to limit overall ionic flux. PorA/C1 rectifies strongly, and this rectification can be accounted for by calculated differences in the voltage and concentration profiles in the access regions. Thus, it appears that the conductance of this channel is determined by the access resistance and the selectivity by a highly-conductive filter.

INTRODUCTION

Membrane channels are structures designed to provide a continuous pathway by which hydrophilic molecules, which are poorly soluble in the hydrophobic membrane environments, cross the membrane. The problem is most formidable for ions whose electric field extends into the medium a distance that is much larger than its ionic radius. Lining the walls of the channel with polar groups and increasing the radius of the water-filled cavity allows more rapid flow by making the inside of the channel more similar to bulk aqueous solution (Parsegian, 1969). However, for the channel to be able to select among possible permeating ions requires some interaction with the walls of the channel. This should slow down ion flow by increasing the time the ion spends in the channel. Thus, in general, highly selective channels would be expected to have a lower conductance than those that are poorly selective.

Here we describe the properties of a channel that is so efficient at allowing ions to permeate that we believe that the rate at which ions reach the selectivity filter is what limits the overall ionic flux. This channel is produced by *Neisseria meningitidis* and is a member of the porin family of proteins (Jeanteur et al., 1991). It has been determined that this species of bacterium can express several such porin proteins that have been categorized into three classes. Although class 2 and class 3 are only weakly selective for anions, class 1 (PorA/C1) is highly selective and yet still highly conductive. The fact that porins exist as trimers forming three aqueous pathways accounts for part of the high conductance. However, we will provide evidence that the nature of the selectivity filter causes it to be virtually nonrate limiting and yet to determine the channel's ion selectivity.

MATERIALS AND METHODS

Bacterial strains, growth conditions, and reagents

The solid typing media and liquid growth media for all the meningococci have been previously described (Porat et al., 1995). The meningococcal strain 44/76 (Δ3Δ4) was provided by Dr. Lee Wetzler (Maxwell Finland Laboratory, Boston City Hospital, Boston, MA) and has been described previously (Guttormsen et al., 1993). All reagents not specifically described were from Sigma (St. Louis, MO).

Isolation and purification of porins

PorA class 1 (PorA/C1) protein from meningococcal strain 44/76 (Δ3Δ4) was isolated using the zwittergen-Ca^{+2} extraction procedure described by Wetzler et al. (1988). Protein concentration was estimated by measuring the absorbance at 280 nm, using an HP Model 8453 UV/Vis rapid scan spectrophotometer equipped with a diode array detector (Hewlett-Packard Company, Palo Alto, CA) with a molar extinction coefficient of 41,960 that was calculated based on class 1 aromatic amino acid content according to Mach et al. (1992).

Polyacrylamide gel electrophoresis

Samples of purified PorA/C1 were incubated with loading buffer containing 0.5% sodium dodecyl sulfate (Novex, San Diego, CA) and either heated at 95°C for 5 min to visualize the porin subunits or maintained at room temperature to observe PorA/C1 oligomers. Electrophoresis was performed using the Tris-glycine buffer and the 8–16% gradient gels obtained from Novex.

Received for publication 20 January 1998 and in final form 15 October 1998.

Address reprint requests to Dr. Marco Colombini, University of Maryland, Department of Biology, College Park, MD 20742. Tel.: 301-405-6925; Fax: 301-314-9358; E-mail: mc34@umail.umd.edu.

0006-3495/99/02/804/10 $2.00

Channel reconstitution

Solvent-free planar phospholipid membranes were produced by a modification (Colombini, 1987) of the monolayer method of Montal and Mueller (1972). Diphytanoylphosphatidylcholine (Avanti Polar Lipids, Inc. Alabaster, AL)/cholesterol (Sigma) 5:1 was used to make the membranes, and the medium was generally 200 mM NaCl. The membrane was voltage clamped, and calomel electrodes were used to interface the electronics with the aqueous phase (Colombini, 1987).

Channels were inserted by adding a 5-μl aliquot of detergent-solubilized PorA/C1 to a 5-ml aqueous phase bathing the membrane while stirring. No channel insertion was observed unless the sample was supplemented with Triton X-100 to a final concentration of 1% (v/v).

Liposome swelling assay

The channel-forming activity of the neisserial porins was assessed by the liposome swelling procedure as described in detail elsewhere (Nikaido et al., 1991; Minetti et al., 1997). The proteoliposomes were prepared using a semisynthetic lipid, dipalmitoyl phosphatidylcholine (Avanti Polar Lipids). The oligosaccharides used in this study were obtained from Sigma and included: L-arabinose (M_r 150); galactose (M_r 180); rhamnose (M_r 182); *N*-acetylglucosamine (M_r 221); sucrose, melibiose, and maltose (M_r 342); raffinose and maltotreose (M_r 504); stachyose (M_r 666); and maltohexaose (990). The rates of permeation of the various sugars into the proteoliposomes was monitored at 450 nm using a Hewlett-Packard Model 8453 UV/Vis rapid scan spectrophotometer equipped with a diode array detector (Hewlett-Packard Company, Palo Alto, CA) and the values expressed as a percent of the rates obtained for L-arabinose.

The Renkin equation (Renkin, 1954) was used to determine the size of the pore following the method of Nikaido et al. (1991).

RESULTS

Single-trimer conductance

Pure PorA/C1 channels were inserted into planar phospholipid membranes composed of uncharged lipids. In near physiological conditions for a mammalian pathogen (200 mM NaCl), the channels inserted in discrete steps (Fig. 1 *A*) that fell into size ranges consistent with single trimers and multiples of the basic trimer conductance (Fig. 1 *B*).

As the channels showed no voltage-gating process, we could not confirm that the single events are indeed trimers but the biochemical characterization shows that the pure channels are trimers. On an sodium dodecyl supfate gel the protein runs as a trimer, and heating the sample results in the formation of monomers (Fig. 2).

The single-trimer conductance, defined as the conductance of the first and major peak of the histogram, increased linearly with increases in the activity of the NaCl of the medium (activities from Robinson and Stokes, 1965). This was determined by examining the conductance of insertion events in mediums with different NaCl concentrations (Fig. 3 *A*) and by adding NaCl to the aqueous phase of membranes containing many channels (Fig. 3 *B*). At high salt, conductance increments are more polydispersed, and this may account for the small deviation from linearity in Fig. 3 *A*. The salt addition experiments were performed in order to circumvent the salt-dependent increase in the variance of the conductance and to extend our measurement to higher NaCl concentrations. Up to 2 M NaCl, the conductance increased essentially linearly with activity.

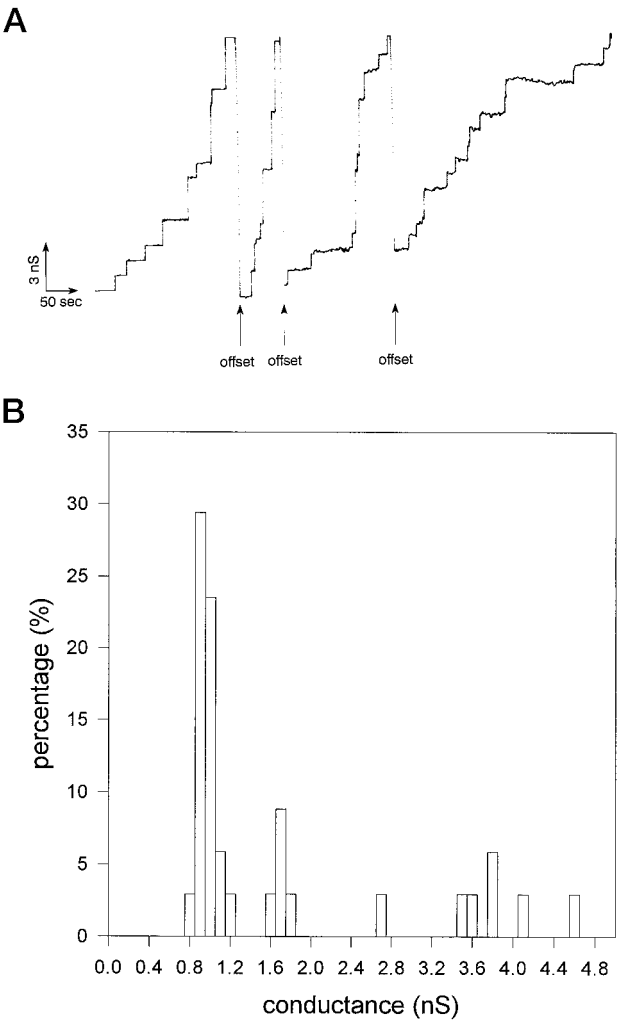

FIGURE 1 Insertion of PorA/C1 channels into planar phospholipid membranes. The pure PorA/C1 protein was added to the aqueous phase (200 mM NaCl) bathing the planar phospholipid membrane (see Methods) and channels spontaneously inserted. The recorded current increments (*A*) were converted to conductance by dividing by the applied voltage (11 mV). Where indicated, the recording was offset in order to keep it in scale. From experiments such as the one illustrated in *A*, insertion increments were quantified and arranged in 0.1 nS bins. The percent of conductance increments in each bin is illustrated in *B*.

PorA/C1 channels show near ideal cation selectivity

In the presence of a twofold gradient of NaCl (200 vs 100 mM), the reversal potential was −15.0 mV. This compares with −16.0 mV for gramicidin (an ideally cation-selective channel) and −16.2 mV for the theoretical value. Buffering the solutions with 1 mM HEPES at pH 7.2 did not change the PorA/C1 reversal potential. Using the Nernst/Planck equation, the permeability ratio for cations over anions is 24 (Table 1).

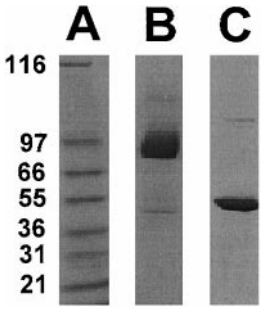

FIGURE 2 Sodium dodecyl sulfate polyacrylamide gel of PorA/C1. *A* contains molecular weight standards. *B* and *C* contain PorA/C1 protein but only the sample in *C* was heated to 95°C.

When this measurement was made in high salt (1.0 vs 0.5 M NaCl), the cation selectivity was weaker but still showed a fivefold preference for Na^+ over Cl^-. The selectivity among cations (K^+ over Na^+) was insignificant.

Effective internal diameter of the aqueous pore

PorA/C1 incorporated into liposomes increases their permeability to sugars as evidenced by a liposome swelling assay (Fig. 4). A pore size of ~1.4 nm was obtained from the relative permeation rates of different sugars. Judging from the nearly identical permeability rates to sucrose, maltose, and melibiose (M_r 342) we may conclude that no specificity to these sugars exist, and the permeation rates rely exclusively on the solute molecular weights. Thus, the estimated pore size should reflect the narrowest portion of the inside of the pore.

Mechanism of permeation

The combination of high cation selectivity and large aqueous pore is consistent with a high density of negative charges in the channel that favors a high concentration of cations in the channel and results in an electrostatic barrier for anions. Such a selectivity mechanism would be expected to show conductance saturation at low salt concentration as the Na^+ concentration in the channel becomes essentially independent of the medium salt concentration.

The channel conductance of class 1 porins did not saturate at low salt concentrations but showed a linear dependence on salt activity. The addition of increasing amounts of NaCl to multichannel membranes caused the conductance to increase linearly from 20 to 60 mM (Fig. 5).

Although the expected saturation was not seen at the salt concentrations examined, the results could be explained if the conductance were limited by the rate of ion access to the highly-charged selectivity filter, not the rate at which ions pass through the selectivity filter. If so, the conductance would depend on the properties of the medium outside the selectivity region such as the medium conductivity.

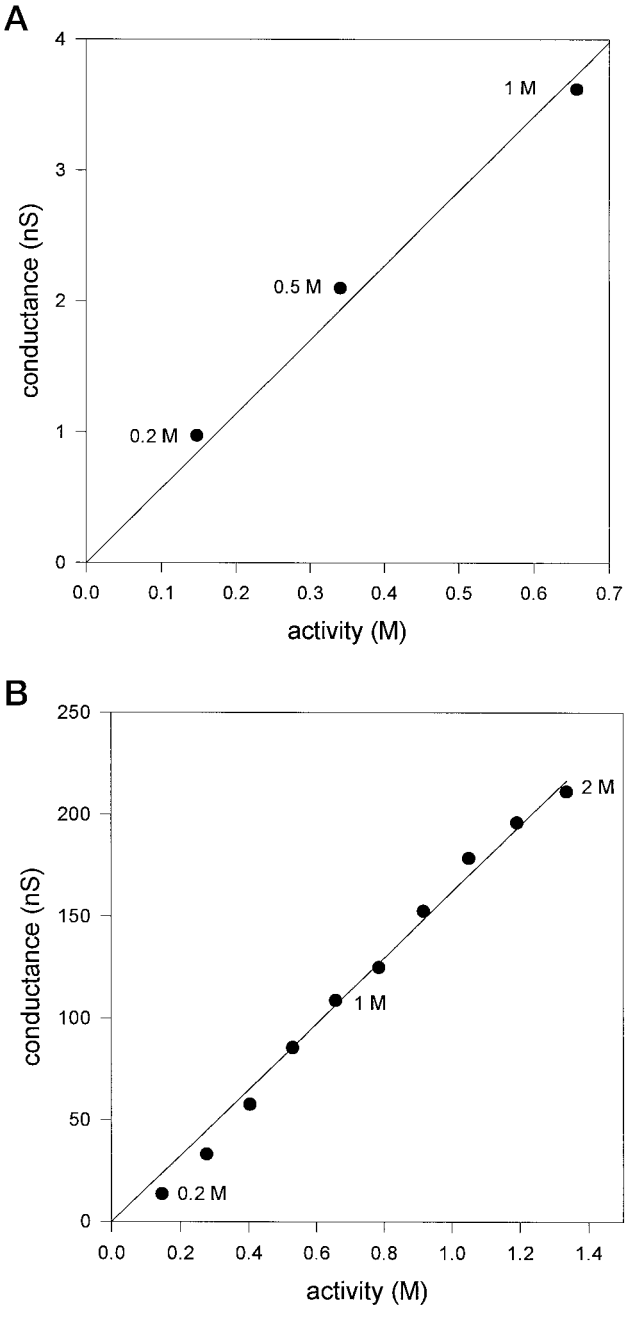

FIGURE 3 The dependence of the conductance of PorA/C1 channels on the medium salt concentration. The smallest group of conductance increments, as illustrated in Fig. 1 *B*, was taken as the distribution of conductances of the single trimer. Similar histograms were generated for 0.5 and 1.0 M NaCl. The means and standard errors of all conductance increments in the smallest group of each histogram were plotted in *A* (error bars were smaller than the point). *B* shows the results of a typical experiment in which the conductance of a multichannel membrane increased incrementally as the NaCl concentration was increased from 200 mM to 2M by additions of 5.0 M NaCl. In both panels, the solid line is the least squares fit forced to go through the origin.

Channel shows strong rectification

PorA/C1 channels show no detectable voltage gating but display pronounced rectification (Fig. 6). Although one

TABLE 1 The reversal potentials (mV, the sign refers to *cis* side) and permeability ratios (P_c/P_a:cation/anion) of gramicidin, PorA/C1, and PorB/C3 proteins in the presence of salt gradients

	Theoretical*		PorA/C1		PorB/C3	
	(mV)	Gramicidin (mV)	(mV)	P_c/P_a	(mV)	P_c/P_a
200 mM NaCl (*cis*) 100 mM NaCl (*trans*)	−16.2	−16.0 ± 0.2 (10)	−15.0 ± 0.3 (11)	24.1	+3.5 ± 0.1 (3)	0.7
200 mM NaCl (*cis*) 100 mM NaCl (*trans*) (pH 7.2)	−16.2	−16.2 ± 0.1 (4)	−15.0 ± 0.1 (5)	24.2	n/a	n/a
200 mM KCl (*cis*) 100 mM KCl (*trans*)	−15.9	−16.1 ± 0.1 (10)	−14.6 ± 0.2 (11)	23.5	n/a	n/a
1 M NaCl (*cis*) 0.5 M NaCl (*trans*)	−16.8	n/a	−11.6 ± 0.2 (3)	5.4	n/a	n/a

*The theoretical reversal potentials for different salt gradients were calculated by using Nernst-Planck equations:

$$\frac{RT}{F}\left(\frac{P_c - P_a}{P_c + P_a}\right)\ln\frac{a2}{a1}$$

in which a2 and a1 are the salt activities of the two solutions (Robinson and Stokes, 1965).

cannot exclude the possibility that these channels gate at very fast rates, the current-voltage relationship shows no hysteresis when recorded at a frequency of 0.1 Hz. The voltage was changing at 100 mV/s. The magnitude of the rectification declined as more channels inserted, and therefore it was recorded soon after the first few insertions. The current at negative potentials was over four times that at positive potentials (Fig. 6, the sign of the potentials refers to the *cis* side).

Theoretical basis for the rectification

A theoretical calculation, yielding the potential profile and ion concentration profile in the access resistance region, provides a plausible explanation for the rectification based solely on a structure for the channel similar to known crystal structures of porins. The use of the simple equation (Hall, 1975) normally used to determine the influence of the access resistance is inappropriate when the ion concentration changes in this region. We used a numerical calculation to determine the changes in potential and ion concentration with distance in the access resistance region. We took the channel to be a cylinder with a 21-Å internal diameter for a 16-strand β barrel (Sansom and Kerr, 1995) and a constric-

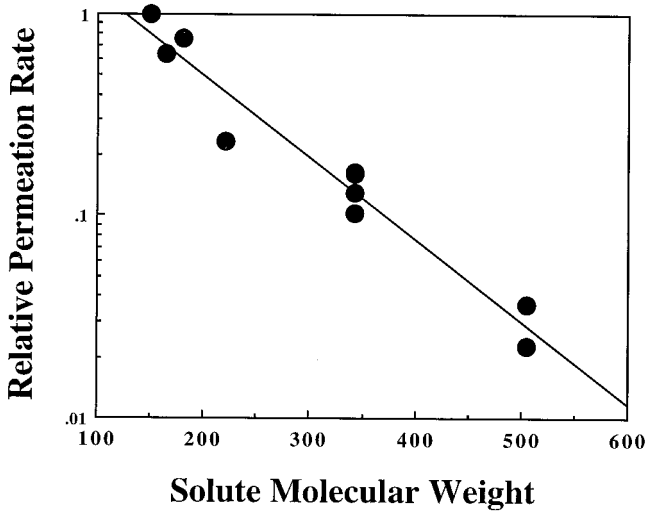

FIGURE 4 Estimation of the effective size of the aqueous pores formed by PorA class 1 protein. Solute dependent permeation rates of proteoliposomes prepared with native class 1 protein. The values are normalized to the permeation rate of L-arabinose and plotted on logarithmic scale. The sugars used are: arabinose (M_r 150); galactose (M_r 180); rhamnose (M_r 182); *N*-acetylglucosamine (M_r 221); sucrose, melibiose, and maltose (M_r 342); and raffinose and maltotreose (M_r 504).

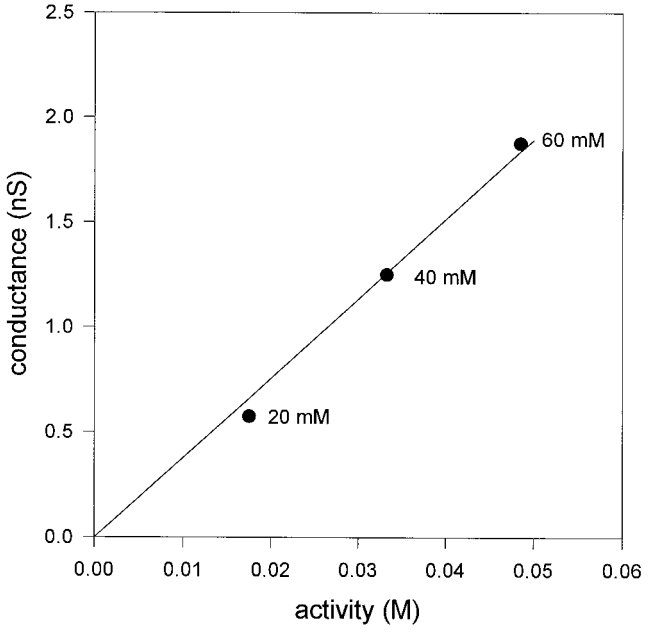

FIGURE 5 Channel conductance varies linearly with NaCl concentration at low concentrations. The membrane was made in the presence of 20 mM NaCl. After a number of channels had inserted and the conductance had stabilized, sufficient 5.0 M NaCl was added to increase the concentration in the chamber to 40 and then to 60 mM. After each increase in salt concentration, the conductance was measured. The measured conductances are plotted as a function of the salt activity.

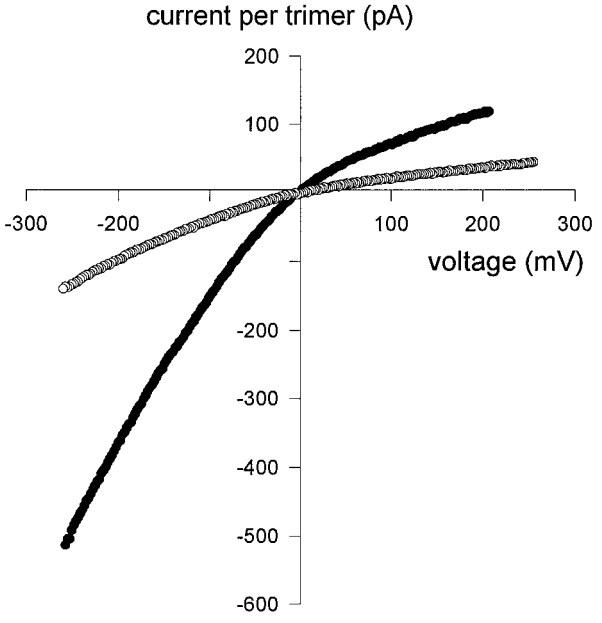

FIGURE 6 The voltage dependence of the current flow through PorA/C1 channels. The current flow through a multiple-channel membrane was recorded by applying 0.1 Hz triangular voltage waves. No hysteresis was detected. The medium was 200 mM NaCl in the absence (*filled circles*) or presence (*open circles*) of 15% PEG 3400 (w/w). The slope of the current between ±10 mV was used to determine the number of trimers in the membrane (using 0.97 nS/trimer). The measured current was divided by the estimated number of trimers. The sign of the potentials refers to the *cis* side.

tion of 14 Å in internal diameter for 1/4 of its length. This constriction would contain the highly charged selectivity filter. Both the wide and narrow pore diameters were reduced by the diameter of a sodium ion (2 Å) to obtain the effective collision cross-section. The model structure is cylindrically symmetrical and so the results can be expressed as distance from the edge of the constricted region.

Starting with the bulk phase 200 Å away, the voltage and concentration of cations and anions was calculated for 0.1-Å increments, using the recorded single-pore current (single-trimer current divided by 3) at ± 250 mV in 200 mM NaCl (filled circles in Fig. 6). Ideal cation selectivity was assumed so that at any point the anion concentration is determined by the local electrical potential. The general Nernst/Planck flux equation was used to relate the observed current (totally attributed to cation flux) to the local cation concentration and the two driving "forces," the ion gradient and the electric field. Within the wide portion of the channel, the solution was divided in 0.1-Å disks. The total current through each disk was

$$I = \pi 6^2 F \mathrm{D}\left(\frac{\Delta c}{\Delta x} + \frac{Fc}{RT}\frac{\Delta \Psi}{\Delta x}\right)$$

in which D is the diffusion constant for Na^+ (1.31×10^{-5} cm^2 s^{-1}), c is the local Na^+, ψ is the local electrical potential, and x is the distance to the selectivity filter. F, R, and T have their usual meaning.

Outside the channel, 0.1-Å thick hemispheres were used, and there the current through each hemisphere was

$$I = 2\pi r^2 F \mathrm{D}\left(\frac{\Delta c}{\Delta r} + \frac{Fc}{RT}\frac{\Delta \Psi}{\Delta r}\right)$$

in which r is the radius of the hemisphere.

The current, reflecting the flux of cations, was maintained constant through all of these segments of solution.

The difference in concentration between the cations and anions was the charge density, and this was used in the Poisson equation to calculate the change in electric field. Within the wide portion of the channel, the one-dimensional Poisson equation was used. We assumed the same dielectric constant as in the bulk phase but the results were not very sensitive to the magnitude of the dielectric constant. Outside the channel, the equation solved for radial symmetry was used (Newman, 1991)

$$\frac{1}{r^2}\frac{\Delta\left(r^2\dfrac{\Delta \Psi}{\Delta r}\right)}{\Delta r} = -\frac{F([\mathrm{Na}^+] - [\mathrm{Cl}^-])}{\epsilon \epsilon_0}$$

in which ϵ is the dielectric constant in 200 mM NaCl (76.3) and ϵ_0 is the permittivity of free space.

The results of the calculations (Fig. 7) show that large changes in the salt concentration and potential occur in the access region in order to maintain the observed current at 250 mV. Fig. 7 *A* illustrates the results of calculations for the case when a positive voltage (+250 mV) is applied to the narrow opening. In this case, the calculation used the high current observed at −250 mV (Fig. 6). The potential is negative on the wide side and thus positive on the narrow side. In Fig. 7 *B*, the positive voltage was applied to the wide opening, and the current used was the lower one observed at +250 mV (Fig. 6). This is positive on the wide side.

The observed currents, while differing by a factor of 4 depending on the direction of ion flow, appear to be the maximum currents that can be supported by the system. The salt concentration declines precipitously as one approaches the pore from the positive potential side and increases rapidly as one approaches from the negative side. The rapid flow through the channel results in ion accumulation on one side and depletion on the other. The "driving force" to maintain the high current comes from a combination of the ion gradient and the electric field. Note in Fig. 7 that the ion concentration on the high-voltage side reaches zero at the entrance to the selectivity filter (solid lines). This indicates that the observed current at each sign of the applied potential is indeed the highest that the access resistance can sustain. If the current used to calculate the profiles in Fig. 7 *A* were used to calculate those in *B*, both the salt concentration and the potential would plunge to negative values, which is impossible.

The asymmetric nature of the channel's structure accounts for the observed rectification. If the channel did not rectify the current, intermediate current levels would be observed at high positive and negative potentials. To obtain

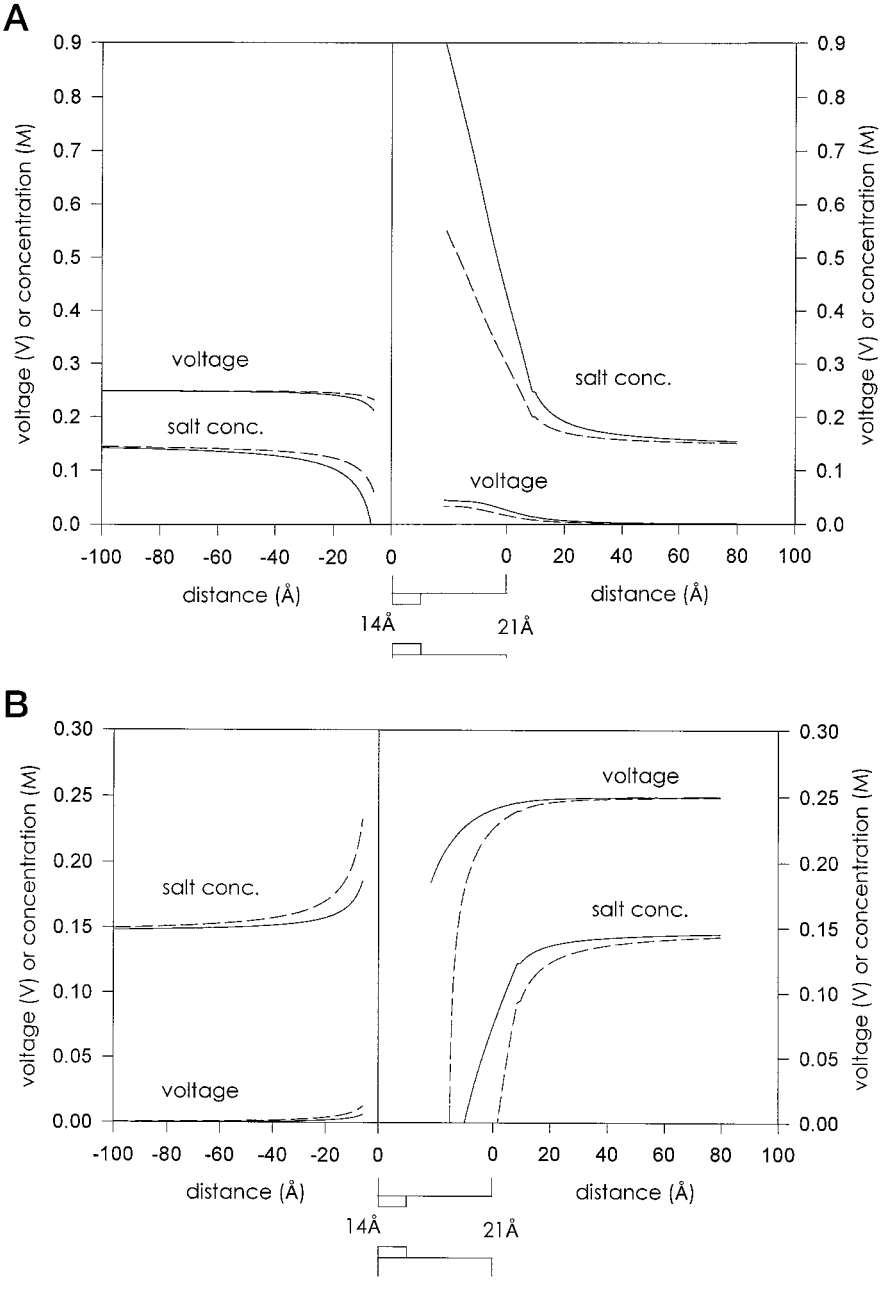

FIGURE 7 The theoretical potential and concentration profiles in the access resistance region. A numerical calculation was used to determine the changes in potential and ion concentration with distance in the access resistance region (see text). The channel was taken to be a cylinder (21 Å in internal diameter with a constriction to 14 Å in internal diameter for 1/4 of its length). This constriction would contain the highly charged selectivity filter. The current used for the solid line was the measured single-pore current (single-trimer current divided by 3) at ±250 mV (*filled circles* in Fig. 6). The salt concentration (*solid lines*) declines precipitously as one approaches the pore from the positive potential side and increases rapidly as one approaches from the negative side. In *A*, the voltage is positive on the constriction side whereas in *B*, it is negative. The dashed lines in the figure are the results of the same calculations if we assume that the channels do not rectify. To do this, the conductance at low voltages was used to calculate the current that would be observed at ±250 mV.

these currents, the conductance at low voltages was used to calculate the current that would be observed at ±250 mV if no rectification took place. The results of calculations using these currents are shown as dashed lines (Fig. 7). In Fig. 7 *B*, the current could not be sustained because both the potential and ion concentration would become negative before reaching the filter. This clearly is not possible. In Fig. 7 *A*, there is no problem but a higher current could be sustained. Thus, this relatively simple calculation shows that the observed currents are likely limited by the access of ions to the selectivity filter and that this limitation can account for the asymmetrical current/voltage relationship.

The direction of the asymmetry depends on the direction of the channels inserted into the membrane. Antibodies were used that are highly specific for one surface of the molecule. With intact cells, they bind almost exclusively to the part of the protein that faces the environment. These antibodies mainly recognize the amino terminus of the molecule including the first proposed loop. According to models of the channel (see Discussion) this region is located on the side of the channel that would likely form the selectivity filter. This end would be the narrow end of the channel. These antibodies reduced the conductance of the channels by 8%. This is a small but reproducible amount. The antibodies also affected the rectification slightly. They only worked when added to the *trans* side (the sign of the potential refers to the *cis* side) indicating that the narrow end of the channel is on the *trans* side. The observed current

was higher when a negative potential was applied to the *cis* side, which should be the wide side. This is consistent with the predictions of the model.

Reduction in bulk-phase conductivity results in a proportional decrease in channel conductance

By using nonelectrolyte polymers that are unable to enter the pore, one can selectively reduce the conductivity of the external medium in order to assess which part of the permeability pathway is rate-limiting. Polyethylene glycol (PEG) of 3400 molecular weight should be unable to enter the pore as it is far greater than the molecular weight cutoff for this channel (700). The addition of this polymer to the salt solution reduces the conductivity by effectively diluting the solution. However, as it is unable to enter the pore, the solution within the pore should be largely unaffected (Bezrukov et al., 1996).

The single-trimer conductance was measured in the presence of 200 mM NaCl with and without 7.5 or 15% (w/w) PEG 3400. The presence of the PEG markedly reduced the conductance, consistent with the hypothesis that the access resistance limits the ion flow through the channel (Fig. 8 *A*). However, the added PEG reduced the single-trimer conductance more than expected by a simple dilution effect of the added PEG. A plot of the single-trimer conductance versus the conductivity of the solution (the filled circles in Fig. 8 *A*) shows a much larger drop in channel conductance than expected from the drop in solution conductivity (the solid line in Fig. 8 *A*). This is especially true for the solution with 15% PEG 3400 in which the conductivity was decreased by half, whereas the channel conductance decreased by almost 80%. The more potent effect on the channels may be caused by the colloidal osmotic pressure exerted by PEG. A negative pressure should be generated (−4.3 atmospheres with 15% PEG) in the channel (at least in the parts totally impermeant to the PEG), and this may somehow reduce the conductance.

To circumvent effects of osmotic pressure, the single-trimer conductance was measured in the presence of 400 mM NaCl containing 15% PEG, a solution whose conductivity is the same at that for 200 mM NaCl (Fig. 8 *B*). The reduced conductance under these conditions must be caused by an action of PEG other than the simple reduction of the conductivity of the external medium. This was used to correct the values obtained in 200 mM NaCl with 15% PEG. Similarly, 300 mM NaCl containing 7.5% PEG had the same conductivity as 200 mM NaCl, and the recorded conductance decrease was used to correct the values obtained in 200 mM NaCl with 7.5% PEG. After the correction, there is still a marked reduction in channel conductance that can only be attributed to a reduction in the conductivity of the external medium. The corrected values (open symbols in Fig. 8 *A*) are close to the expected line if the external medium conductivity were the only rate-limiting step.

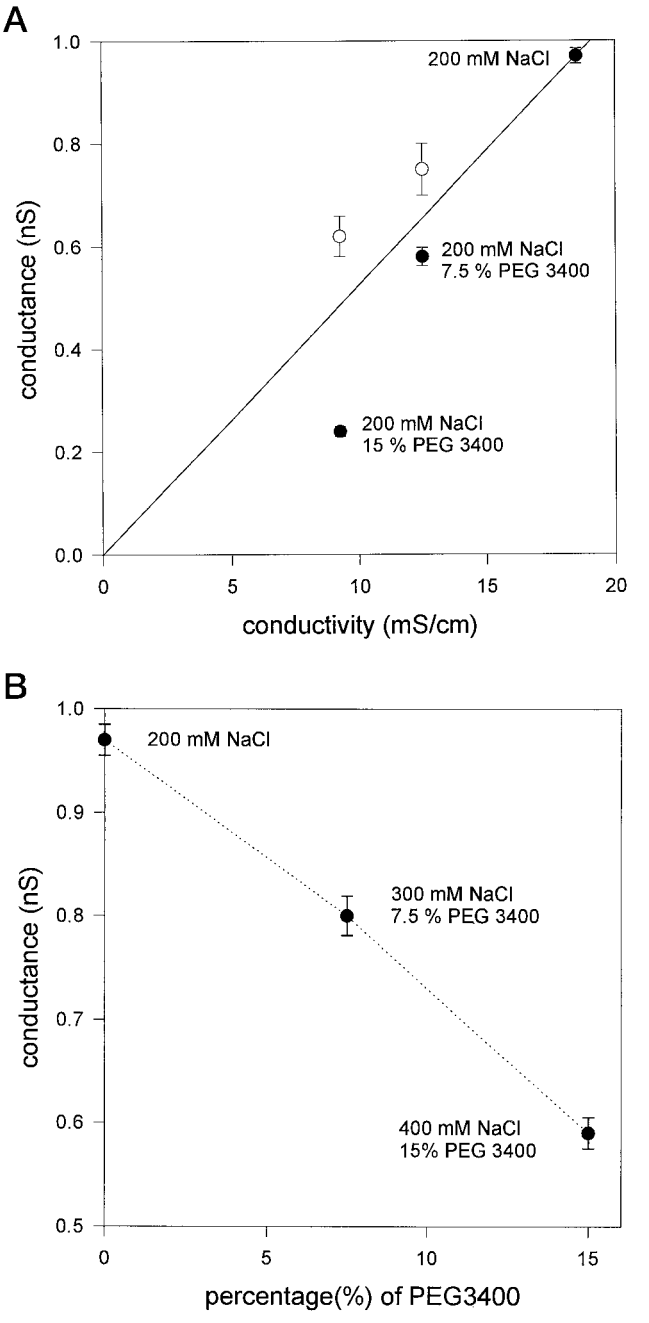

FIGURE 8 Uncharged impermeable polymers reduce the conductance of PorA/C1 channels. Histograms, as shown in Fig. 1 *B*, were generated for insertions in the presence of 200 mM NaCl and either 7.5% (w/w) or 15% (w/w) PEG 3400 (*A*). The group of conductance increments, representing single-trimer insertions, were averaged and plotted in *A* along with the conductance in the absence of PEG (*filled circles*) against the measured bulk conductivities of these solutions. The open circles are corrected values of the PEG results. Each was corrected by adding an amount equal to the decrease in single-trimer conductance in the presence of 300 mM NaCl with 7.5% PEG 3400 or 400 mM NaCl with 15% PEG 3400 (*B*), as appropriate. This allowed for corrections of what are believed to be osmotic effects of PEG. The line, indicating the theoretical single trimer conductance as a function of medium conductivity, was obtained by connecting the conductance recorded for 200 mM NaCl without PEG with the origin. The error bars are standard errors of the mean.

TABLE 2 The rectification of currents through PorA/C1 in the absence and presence of PEG3400

	Slope conductance (nS)			Rectification
	Low potential	High negative	High positive	High negative/High positive
200 mM NaCl	0.97	2.48	0.44	5.7
200 mM NaCl + 15% PEG 3400	0.24	0.68	0.12	5.5
Percent decrease with PEG 3400	75%	73%	73%	3%

The presence of 15% PEG 3400 reduced the current flow at all potentials by the same factor, ~73%. Thus, the PEG did not affect the rectification (Fig. 6 and Table 2).

DISCUSSION

A porin composed of PorA/C1 protein seems to have generated a selectivity filter that is so efficient at conducting cations that the filter does not significantly limit the channel conductance. The filter imparts high selectivity for cations over anions under the conditions the bacterium might find when it infects the nervous system. This is achieved simultaneously with the high throughput. We propose that channel conductance is determined exclusively (within experimental limitations) by the ability of ions to reach the filter, i.e., the access resistance.

The evidence for these assertions comes mainly from the electrophysiological properties of the channels. In order to achieve both high selectivity and high throughput of small ions with an aqueous pore 1.4 nm in diameter, one might expect a selectivity filter containing a high charge density. Such a structure would maintain a high concentration of mobile ions, Na^+ in this case. This high concentration of Na^+ would make the channel conductance less sensitive to salt concentration, especially at low salt concentrations. However, experiments demonstrate that the conductance changes linearly with salt concentration from 20 mM to 2M NaCl. This is remarkable and inconsistent with a highly-charged selectivity filter determining the channel conductance. However, if the access resistance was rate limiting, its conductance should change linearly with salt concentration.

The average conductance of the unitary insertion event, the presumptive trimer, is 0.97 nS (in 200 mM NaCl). Thus a single pore should conduct at 0.33 nS, assuming no competition between the single pores for incoming ions. This high conductance is further increased when a negative potential is applied to the *cis* compartment. The antibody experiments indicate that the channels orient in the membrane is such a way that the *cis* compartment would be the periplasmic space. Thus, the channels are oriented in vivo in such a way that voltages that drive cations into the cell produce higher ion fluxes than those that drive ions out of the cell.

The observed currents correspond to fluxes that are extraordinarily large. The flux of Na^+ at −250 mV is higher than the maximum flux calculated from the infinite sink

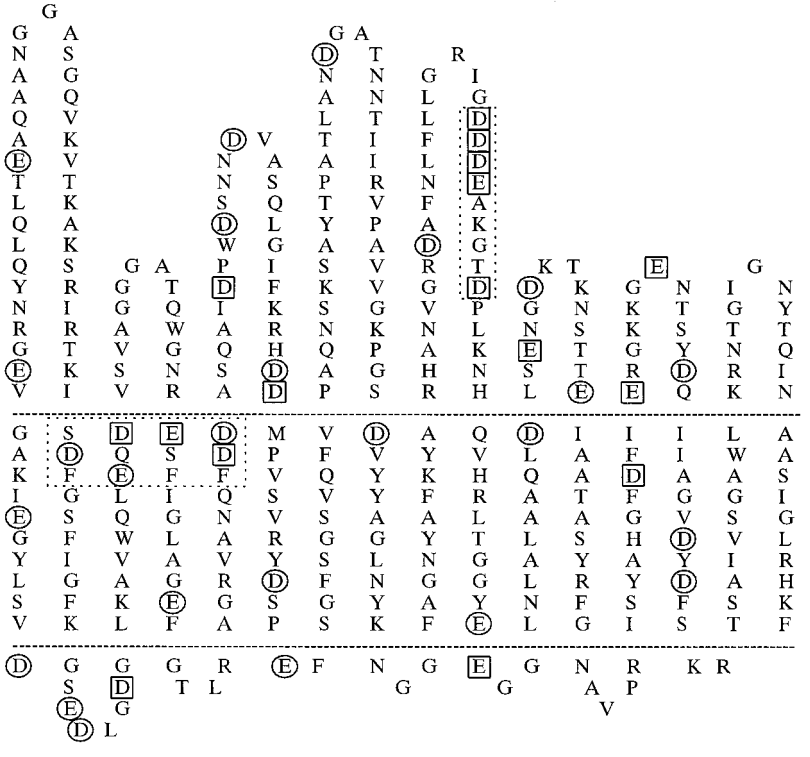

FIGURE 9 Proposed folding pattern of PorA/C1 in the membrane. The folding pattern was taken from van der Ley et al. (1991). The horizontal dashed lines illustrate the limits of the transmembrane region. The lower portion would be the periplasmic space and the upper, the extracellular space. Amino acid residues with negative side chains are either boxed or circled. The residues corresponding to the boxed residues are either absent or uncharged in PorB/C3. The dotted boxes identify two regions enriched in negative charge that we propose form the selectivity filter.

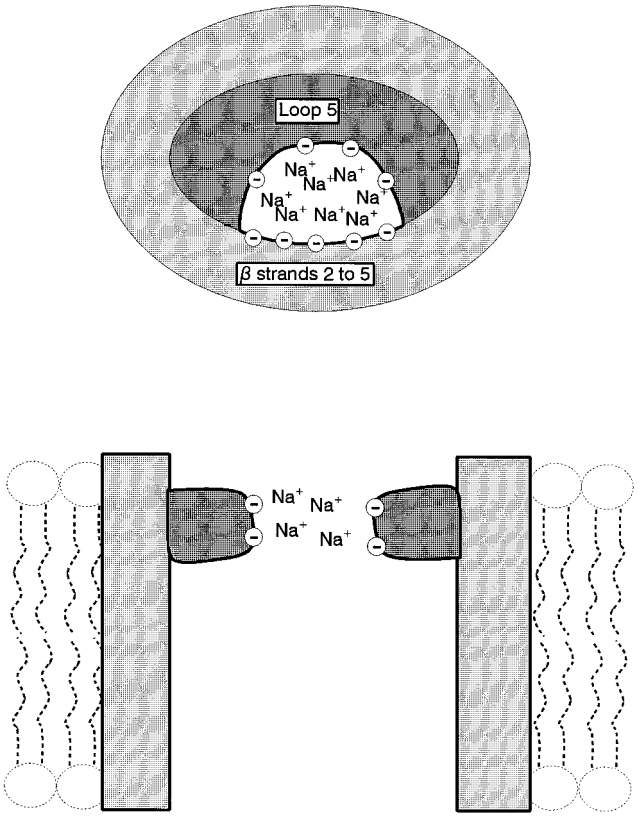

FIGURE 10 Proposed structure of PorA/C1. Longitudinal section (*lower*) and cross-section through the selectivity filter (*upper*) of the proposed basic structure of PorA/C1. In the lower figure, the upper portion would face the extracellular space and the lower, the periplasmic space. Loop 5 is proposed to fold into the pore, occluding part of the space, and contributing negative charges to the constricted, selectivity filter region. Charged portions of β-strands 2 to 5 would also form part of this filter. The charged residues would form a negative potential well that would contain a high concentration of mobile Na^+ counterions. Anions would tend to be excluded. The mobile cations would make this region highly conductive.

equation (1.2×10^9 ions/s per single pore versus 7×10^8 ions/s for a pore with a diameter of 14 Å). This indicates that the channels process ions so rapidly that gradients of potential must develop in the medium that accelerate ion flow toward the "infinite sink."

After correction for what are likely osmotic effects of PEG 3400, the channel conductance still declined as the conductivity of the external medium was reduced by PEG 3400 addition. It has been shown for other channels (Bezrukov et al., 1996) that permeating nonelectrolytes reduce the conductance of the channel while nonpermeating nonelectrolytes if anything somewhat increased the conductance by binding water and increasing the salt activity. In the case of PorA/C1, the impermeant nonelectrolyte decreases the conductance. This is consistent with ion flow through the solution outside the channel being the rate-limiting step. The corrected conductance was higher than expected if the entire conductance were strictly determined by the properties of the PEG-containing bulk phase. However, a vestibule-like portion of the channel that is outside the selectivity filter region would probably be inaccessible to PEG 3400 and thus be unaffected by PEG addition. Thus, while not the ideal result, these findings argue strongly for access to the channel being the rate-limiting step.

PorA/C1 and PorB/C3 are closely-related channel-forming proteins both produced by *N. meningitidis*. Despite their sequence similarity, the selectivity of these channels is very different. PorA/C1 is highly cation selective and PorB/C3 is poorly selective for anions. A comparison of the sequences of PorA/C1 with that of PorB/C3 reveals many charge changes. Although there are both changes that result in an increase in negative and positive charge, the former outnumber the latter. More importantly, the changes occur in clusters. All changes that resulted in the formation of a negative charge are boxed in Fig. 9. The remaining negative charges are circled. Note the accumulation of negative charge in the regions outlined with the dotted lines. The amino-acid sequence is shown folded in a previously-proposed folding pattern (van der Ley et al., 1991). The regions containing clusters of negative charges are located at one end of β strands 2 to 5 and in loop 5. Together, these regions carry a net charge of -10 elementary charges.

The known three-dimensional crystal structures of porins reveal that a loop or loops extend within the channel, constricting the pathway. This constriction has been shown to be very important in channel selectivity. The loop or loops involved in forming this constriction vary from porin to porin. To our knowledge, loop 5 has not been identified as the constriction loop in other porins, but we propose that it performs this function in PorA/C1. Evidence for this proposal comes from closely related channels expressed by *N. gonorrhea*, i.e., PIb and PIa. Gonococcal PIb porins contain two trypsin susceptible cleavage sites within loop 5 (Blake and Gotschlich, 1983). PIb is selective for anions at a ratio of 6 to 1 (Greco, 1981), but this selectivity is markedly reduced by treatment of the reconstituted channels with trypsin (Greco, 1981). An additional indication is the fact that PorA/C1 contains a string of four adjacent negatively charged residues within loop 5, which are not found in the related PorB/C2 or PorB/C3. We propose that this, along with the charges present at the ends of β strands 2 to 5 form the selectivity filter (Fig. 10). Note that other parts of the β-strand wall are too far from the constricted filtering region to affect ion selectivity. Thus, by proposing a structure in analogy with solved porin crystal structures, we can generate a very narrow and highly negatively charged selectivity filter.

The high negative charge on the filter would be accompanied by a high local Na^+ concentration. This high concentration can account for both the high selectivity and the high conductance of the filter itself. A simple calculation should suffice. The conductance of the filter region can be estimated by limiting the charge carrier to Na^+ and determining the amount present from the estimated amount of fixed negative charge. If the constriction in the filter region is 1 nm thick, 8 to 10 Na^+ ions result in a conductance between 66 and 83 nS. This is 20-fold greater than the

highest observed conductance for a single trimer and thus ~60-fold higher than that of 1 pore. Thus, the selectivity filter need not provide any significant limitation to ion flow.

The rectification of the current can be understood in terms of the proposed structure (Fig. 10). The calculations of the salt concentration changes, and the potential changes in the medium (Fig. 7) show that the access resistance region may limit ion flow through this channel. Using a model based on the known structures of porins, the calculations show that the observed currents are just about the maximal currents that could be supported by the access resistance regions. The asymmetrical current at positive and negative potentials is also consistent with the model. The antibodies, which are specific for a domain on the side of the channel that contains the loop region that might form the selectivity filter, indicate that the channels insert in such a way that the narrow portion faces the *trans* side. If so, the wide side is on the *cis* side, and a negative potential on the wide side does result in higher current. This is consistent with the mathematical model and with its premise that the access resistance region limits the current and is responsible for the observed rectification.

The mathematical model used assumed the existence of only one pore. Like most porins studied, class one is a trimer. The proximity of three pores will clearly cause more depletion of the salt concentration at the mouth of the channel. We did not calculate the effect of this added depletion but expect it to be minor because the distance between the pores is about 90 Å. The hemispheres that were used to calculate the axis resistance of one pore would only begin to overlap with hemispheres of adjacent pores when the distance from the mouth of the channel was 45 Å. Therefore, the pores are spaced far enough apart to minimize cross-talk.

It must be pointed out that PorA/C1 is not unique in having a high selectivity. Other porins have been reported (Benz et al., 1985) to have high selectivity, and thus the current through these channels may also be limited by the access resistance. It is doubtful that PorA/C1 is unique in this regard.

One can only speculate as to why a bacterium might want a highly-selective and highly conductive channel in its outer membrane. It should be pointed out that in the strains of *N. meningitidis* studied to date, PorA/C1 has not been found in homotrimers but as one pore in a heterotrimer. The other pores are PorB/C3 that form poorly selective channels. In any event, from a biophysical viewpoint, PorA/C1 homotrimer is very well designed. A relatively small amount of protein is used to form three parallel pathways. Each pathway is constricted in a very small location (based on crystal structures of other porins) at which a high charge density is focused to achieve high selectivity and high conductance. The constriction is kept away from the thin protein wall to keep the permeating ions away from the low dielectric constant environment of the phospholipids. Thus, the channel is well-designed and well-suited for high selectivity and high ion flow. One can only assume that strong selection pressures have resulted in this compact and highly efficient structure.

REFERENCES

Benz, R., A. Schmid, and R. W. Hancock. 1985. Ion selectivity of Gram-negative bacterial porins. *J. Bacteriol.* 162:722–727.

Bezrukov, S. M., I. Vodyanoy, R. A. Brutyan, and J. J. Kasianowicz. 1996. Dynamics and free energy of polymers partitioning into a nanoscale pore. *Macromolecules.* 29:8517–8522.

Blake, M. S., and E. C. Gotschlich. 1983. Progress in Allergy, Vol. 33. Karger, Basel. 298–313.

Colombini, M. 1987. Characterization of channels isolated from plant mitochondria. *In* Methods in Enzymology. Vol. 148. L. Packer and R. Douce, editors. Academic Press, New York. 465–475.

Greco, F. 1981. The formation of channels in lipid bilayers by gonococcal major outer membrane protein. Thesis, Rockefeller University, New York.

Guttormsen, H. K., L. M. Wetzler, and A. Naess. 1993. Humoral immune response to the class 3 outer membrane protein during the course of meningococcal disease. *Infect. Immun.* 61:4734–4742.

Hall, J. E. 1975. Access resistance of a small circular pole. *J. Gen. Physiol.* 66:531–532.

Jeanteur, D., J. H. Lakely, and F. Pattus. 1991. The bacterial porin superfamily: sequence alignment and structure prediction. *Molec. Microbiol.* 5:2153–2164.

Mach H., C. R. Middaugh, and R. V. Lewis. 1992. Statistical determination of the average values of the extinction coefficients of tryptophan and tyrosine in native proteins. *Anal. Biochem.* 200:74–80.

Minetti, C. A. S. A., J. Y. Tai, M. S. Blake, J. K. Pullen, S. M. Liang, and D. P. Remeta. 1997. Structural and functional characterization of a recombinant PorB class 2 protein from Neisseria meningitidis: conformational stability and porin activity. *J. Biol. Chem.* 272:10710–10720.

Montal, M., and P. Mueller. 1972. Formation of bimolecular membranes from lipid monolayers and a study of their electrical properties. *Proc. Natl. Acad. Sci. USA.* 69:3561–3566.

Newman, J. S. 1991. Electrochemical Systems. Prentice Hall, Englewood Cliffs, New Jersey. 87.

Nikaido, H., K. Nikaido, and S. Harayama. 1991. Identification and characterization of porins in Pseudomonas aeruginosa. *J. Biol. Chem.* 266: 770–779.

Parsegian, A. 1969. Energy of an ion crossing low dielectric membrane: solutions four relevant electrostatic problems. *Nature.* 221:844–846.

Porat, N., M. A. Apicella, and M. S. Blake. 1995. A lipooligosaccharide-binding site on HepG2 cells similar to the gonococcal opacity-associated surface protein Oka. *Infect. Immun.* 63:2164–2172.

Renkin, E. M. 1954. Filtration, diffusion, and molecular sieving through porous cellulose membranes. *J. Gen. Physiol.* 38:225–243.

Robinson, R. A., and R. H. Stokes. 1965. Electrolyte Solutions. Butterworths, London. 492–494.

Sansom M. S. P., and I. D. Kerr. 1995. Transbilayer pores formed by β-barrels: molecular modeling of pore structures and properties. *Biophys. J.* 69:1334–1343.

van der Ley, P., J. E. Heckels, M. Virji, P. Hoogerhout, and J. T. Poolman. 1991. Topology of the outer membrane porins in pathogenic *Neisseria* spp. *Infect. Immun.* 59:2963–2971.

Wetzler L. M., M. S. Blake, and E. C. Gotschlich. 1988. Characterization and specificity of antibodies to protein I of *Neisseria Gonorrhoeae* produced by injection with various protein I-adjuvant preparations. *J. Exp. Med.* 168:1883–1897.